Cell response to a newly developed Ti-10Ta-10Nb alloy and its sputtered nanoscale coating

Young-Min Kim[1], DDS, Mong-Sook Vang[2], DDS, MSD, PhD, Hong-So Yang[2], DDS, MSD, PhD, Sang-Won Park[2]*, DDS, MSD, PhD, Hyun-Pil Lim[3], DDS, MSD

[1]Graduate Student, [2]Professor, [3]Clinical Professor, Department of Prosthodontics, Graduate School, Chonnam National University

STATEMENT OF PROBLEM. The success of titanium implants is due to osseointegration or the direct contact of the implant surface and bone without a fibrous connective tissue interface. **PURPOSE**. The purpose of this study was to evaluate the osteoblast precursor response to titanium - 10 tantalum - 10 niobium (Ti-Ta-Nb) alloy and its sputtered coating. **MATERIAL AND METHODS**. Ti-Ta-Nb coatings were sputtered onto the Ti-Ta-Nb disks. Ti6-Al-4V alloy disks were used as controls. An osteoblast precursor cell line, were used to evaluate the cell responses to the 3 groups. Cell attachment was measured using coulter counter and the cell morphology during attachment period was observed using fluorescent microscopy. Cell culture was performed at 4, 8, 12 and 16 days. **RESULTS**. The sputtered Ti-Ta-Nb coatings consisted of dense nanoscale grains in the range of 30 to 100 nm with alpha-Ti crystal structure. The Ti-Ta-Nb disks and its sputtered nanoscale coatings exhibited greater hydrophilicity and rougher surfaces compared to the Ti-6Al-4V disks. The sputtered nanoscale Ti-Ta-Nb coatings exhibited significantly greater cell attachment compared to Ti-6Al-4V and Ti-Ta-Nb disks. Nanoscale Ti-Ta-Nb coatings exhibited significantly greater ALP specific activity and total protein production compared to the other 2 groups **CONCLUSIONS**. It was concluded that nanoscale Ti-Ta-Nb coatings enhance cell adhesion. In addition, Ti-Ta-Nb alloy and its nanoscale coatings enhanced osteoblast differentiation, but did not support osteoblast precursor proliferation compared to Ti-6Al-4V. These results indicate that the new developed Ti-Ta-Nb alloy and its nanoscale Ti-Ta-Nb coatings may be useful as an implant material. **KEY WORDS**. Implant, Ti-Ta-Nb, Cell response, Sputter, Nanoscale, Osteoblast **[J Adv Prosthodont 2009;1:56-61]**

INTRODUCTION

Titanium (Ti) and its alloys have been widely used in dental and orthopedic fields as biomaterials. The success of titanium implants depends on osseointegration or the direct contact of the implant surface and bone without a fibrous connective tissue interface, where the Ti contacting bone is a very thin layer of amorphous titania (TiO_2). The initial interaction occurs at the bone implant surface after surgical insertion largely responsible for successful bone formation. Bone formation on an implant surface requires recruitment of osteoblast precursor cells, their differentiation into secretory osteoblast, production of unmineralized extracellular matrix (osteoid), and calcification of the extracellular matrix.[1]

Because rapid adsorption of proteins is the first event occurring when a foreign material is implanted, the investigation of protein adsorption on implant surfaces needs to be critically evaluated. *In vitro* cell culture studies, the ALP-specific activity and osteocalcin level, are used as markers for determining osteoblast phenotype and are considered to be important factors in determining bone mineralization. Cells grown on media containing high and low Ca^{2+} were observed to exhibit a significantly higher ALP specific activity over the course of the study, indicating greater cellular differentiation.

Recently, *in vitro* cellular models osteoblast proliferation, differentiation and mineralization are greater on sintered nanoscale crystal TiO_2 bulk ceramics than on conventional microscale formulations of the same ceramics.[2] It was hypothesized in this study that nanoscale crystal TiO_2 coating on Ti implant enhances osteoblast activity and there exists an optimal nanoscale crystal size.

Although titanium - 6% aluminum - 4% vanadium (Ti-6Al-4V) alloy has been widely used as a implant material in dentistry and orthopedics, there are some concerns about the presence of vanadium and aluminum with respect to cytotoxicity, neurotoxicity and dementia.[3-5] In order to avoid the use of vanadium and aluminum in implant devices, other new titanium alloys for biomedical applications have been developed[6,7] and included in ASTM standardization. These new titanium alloys contain non-toxic elements such as tantalum (Ta)[8-15] and niobium (Nb). Tantalum and niobium derived medical devices have been used as stents,[16-18] suture[19] and bone repair scaffolds[20-22] in clinics. A three-dimensional Ta-coated porous biomaterial improved an *in vitro* preservation of progenitor viability and multipotency.[23] A new titanium - 10 tantalum - 10 niobium (Ti-Ta-Nb) system alloys have developed for dental and orthopedic applications. The newly developed Ti-Ta-Nb alloys have excellent mechanical and corrosion resistance properties similar to those of Ti-6Al-4V alloy and commercially pure titanium. However, the biocompatibility

Corresponding author: Sang-Won Park
Department of Prosthodontics, School of Dentistry, Chonnam National University
300 Yongbong-dong, Buk-gu, Gwang-Ju, 500-070, Korea
Tel, +82 62 530 5638: e-mail, psw320@chonnam.ac.kr

Received January 28, 2009/ Last Revison February 24, 2009/ Accepted March 3, 2009

of the newly developed Ti-Ta-Nb alloy is largely unknown. In addition, no investigation on the influence of nanoscale Ti-Ta-Nb coatings with respect to biological responses has been reported in the literature.

In this study, surface characteristics for Ti-10Ta-10Nb alloy and its sputtered nanoscale crystal coating were evaluated. Ti-10Ta-10Nb alloy and its sputtered nanoscale crystal coating were evaluated surface characteristics. Then, the cell proliferation, differentiation, attachment, morphology, dsDNA assay and total protein production assay were observed.

MATERIAL AND METHODS

Material

In our study, three different surfaces were prepared as follows: (1) cast Ti-Ta-Nb disks(weight percentage: 10% Ta, 10% Nb, and Ti balance) of 15 mm diameter and 2 mm thickness, (2) sputtered Ti-Ta-Nb coatings on Ti-Ta-Nb disks, and (3) non-coated Ti-6Al-4V disks of 15 mm diameter and 2 mm thickness as controls. The Ti-6Al-4V and Ti-10Ta-10Nb disks were wet ground with 240, 400 and 600 grit silicon carbide papers. These surfaces were ultrasonically degreased in acetone and ethanol for 10 minutes each, with deionized water rinsing between applications of each solvent. A passivation procedure was conducted by exposing the Ti samples to a 40% volume nitric acid solution at room temperature for 30 minutes (ASTM F86-91). After each surface treatment, the Ti samples were rinsed with deionized water. Deposition of the Ti-Ta-Nb coating on the Ti-Ta-Nb disks was performed using a CMS-18 radiofrequency magnetron sputtering system (Kurt J Lesker Company, Clairton, PA, USA), at a pressure of 1.0 - 1.5 mbar, and a sputtering power of 300 W for 15 minutes (coating rate of 1 ㎛/hour), and using a 4 inch Ti-Ta-Nb target. Prior to the experiment, all samples were sterilized using gas polyethylene oxide (PEO).

X-ray diffraction (XRD)

A D8 Advanced x-ray diffractometer (Bruker, Wisconsin, USA), equipped with a single Gobel mirror to yield a diffracted parallel beam while removing the $K\beta$ radiation, was used to characterize the structure of disks and coatings. Using a grazing incidence attachment, a 0.35° soller slit and a LiF (100) flat crystal monochromator to improve resolution and peak-to-background ratios, triplicate coatings were analyzed using Cu K radiation at 40 KV and 30 mA. Triplicate samples per group were scanned from 20° to 80° 2θ at a scan rate of 0.1° per minute.

Scanning electron microscope (SEM)

Surface morphology of the samples was observed using a S-4200 scanning electron microscope (Hitachi, Japan). Sputtered coating was deposited on glass substrate and the cross section morphology of coating was observation with fracturing coated glass. Triplicate samples were then evaluated using a SEM with an acceleration voltage of 15 KV to 20KV.

Cell culture

The cell culture study was conducted over a 16-day period. Surfaces were seeded with 50,000 cells per sample in a 24 well plate. One ml of the DMEM containing 7% fetal bovine serum, 1% antibiotic-antimycotic solution, and 50 μg/ml ascorbic acid and 4 mM β-glycerophosphate was added per well of a 24 well plate containing one of the three groups listed above. The cells were incubated at 37℃ in a humidified atmosphere of 95% air and 5% CO_2. The culture media were changed once for four days with DMEM media. On days 4, 8, 12, and 16, the supernatants were collected and surfaces were washed twice with a phosphate buffered solution. The cells were then be lysed using 0.5 ml 0.2% Triton-X-100 solution (Fisher Scientific, Houston, USA) and stored at -20℃ until assayed.

Cell attachment study

The initial cell attachment study was conducted using the American Type Culture Collection (Manassas, VA, USA) CRL 1486 human embryonic palatal mesenchyme (HEPM) cells, an osteoblast precursor cell line. The cells were incubated in Dulbecco's modified Eagle's medium (DMEM) containing 7% FBS, penicillin (5000 unitsml^{-1}), and streptomycin (5000 gml^{-1}), and fungizone (250 g/ml) in a 5% CO_2 humidified incubator at 37℃. Osteoblasts from pre-confluent cultures were harvested with 0.25% trypsin - 1 mM EDTA (GibcoBRL, life Technologies, NY), then centrifuged and produced to cell suspension with DMEM. The cells were seeded onto the samples in 24 well culture plates at a density of 50,000 cells on each sample and incubated in a 5% CO_2 humidified incubator at 37℃ for 30, 60, 120, 240 and 360 minutes. At each time period, the non-adherent cells at five sample/group were removed and washed twice using phosphate buffered solution. The non-adherent cells in the removed and wash solution were counted using a coulter counter (Z2, Beckman Coulter. Inc.). The cell attachment was determined by subtracting the residual cell from the initial cell concentration seeded. Mean attachment cell concentrations between the different surfaces were statistically analyzed using the One-Way ANOVA test, and differences considered significant if $P < .05$.

Cell morphology

The adherent cells on the samples over time were labeled using dye DiI (Vybrant Cell-labeling solution, Molecular Probes, Eugene, OR) and observed using fluorescent microscope (TE2000U, Nikon Instruments Inc.).

dsDNA assay

dsDNA was quantified via PicoGreen assay (Molecular

Probe, Gene, OR), which indicates the cell proliferation. Differences in dsDNA were statistically compared using the ANOVA test (*P* < .05), with differences assessed using the Tukey's multiple comparison test.

Alkaline phosphatase (ALP) activity

Five samples/per group/time period were used for measuring the alkaline phosphatase activity. The cell lysates (50 μl) were added to 50 μl of working reagent (1.5 M 2-amino-2 methyl-1-propanol, 20 mM p-nitrophenol phosphate, and 1 mM magnesium chloride). The samples were then be incubated for 3 hours at 37℃. After 3 hours incubation, the reaction was stopped with the addition of 100 μl of 1 N NaOH and read using a Titertek Multiscan Plus MK II microplate reader (MTX Labsystems, Inc, VA, USA) at 405 nm. The absorbance for the cell layer suspension were correlated to a standard ALP activity curve prepared using p-nitrophenol stock standard. The ALP specific activity was calculated by normalizing the ALP activity to dsDNA produced from each sample. Differences in ALP specific activity were statistically compared using the ANOVA test (*P* < .05), with differences assessed using the Tukey's multiple comparison test.

Total protein production assay

Five samples/per group/time period were analyzed for total protein synthesis. Protein synthesis analysis was performed using the Pierce BCA protein assay kit (Pierce, IL). The cell lysates (30 μl) were added to 200 μl of working reagent (sodium carbonate, sodium bicarbonate, BCA detection reagent, sodium tartrate in 0.1 M NaOH, and 4% copper sulfate). The samples were incubated for 30 minutes at 37℃ and read using a microplate reader at 600 nm. The absorbance for the cell lysates were correlated to a standard protein curve and differences in protein synthesis statistically compared using the ANOVA test (*P* < .05), with differences assessed using the Tukey's multiple comparison test.

RESULTS

X-ray diffraction (XRD)

The thin film XRD pattern of the Ti-6Al-4V disks, Ti-Ta-Nb disks, and sputtered Ti-Ta-Nb coatings on Ti-Ta-Nb disks (Fig. 1).

Scanning electron microscope (SEM)

The three surfaces exhibited the same alpha-Ti crystal structure. SEM showed that the Ti-6Al-4V (Fig. 2a) and Ti-Ta-Nb disks (Fig. 2b) exhibited microgroove due to polishing and the sputtered Ti-Ta-Nb coating consisted of irregular nanoscale grains in the range of 30 to 100 nm (Fig. 2c). The cross-section surface of the sputtered Ti-Ta-Nb coatings exhibited a very dense columnar structure (Fig. 2d).

Cell attachment study

The cell attachment kinetics of different surfaces. The cell adhesion on all the surfaces greatly increased after the first two hours and reached a plateau after the first four hours (Fig. 3). The sputtered nanoscale Ti-Ta-Nb coatings exhibited significantly greater cell attachment compared to Ti-6Al-4V disks (*P* < .01) and Ti-Ta-Nb disks (*P* < .05). There were no significant differences between the Ti-Ta-Nb and Ti-6Al-4V disks.

Cell morphology

The representative morphology change of the adherent cell on the samples over time (Fig. 4). After the first hour, the adherent cell exhibited round shape. After the first two and four hours, the adherent cell increased in area and gradually elongated over time, suggesting the cell's continuing adherence. After the first

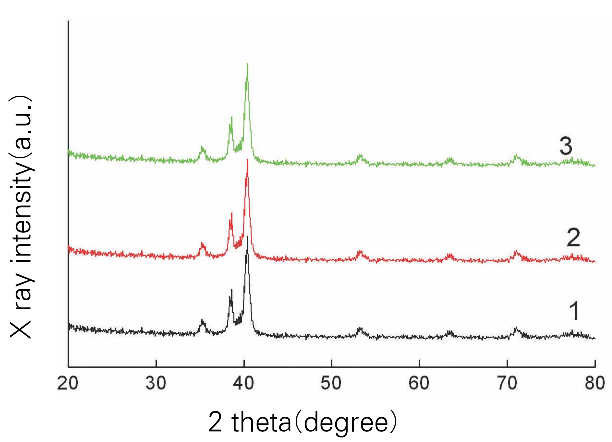

Fig. 1. Thin film XRD pattern of (1) Ti-6Al-4V controls; (2) Ti-Ta-Nb disks; and (3) Sputtered Ti-Ta-Nb coatings on Ti-Ta-Nb disks. The three surfaces exhibited the same alpha-Ti crystal structure.

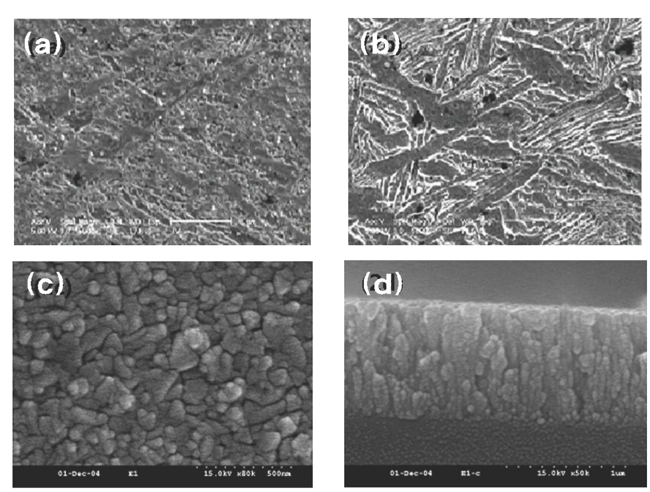

Fig. 2. Surface morphology of (a) Ti-6Al-4V controls; (b) Ti-Ta-Nb disks; and (c) Sputtered Ti-Ta-Nb coatings on Ti-Ta-Nb disks. (d) Cross-section surface morphology of the sputtered Ti-Ta-Nb coatings.

six hours, the adherent cell exhibited the spindle shape and projected some visible filopodia, suggesting the start of spread.

dsDNA assay

The dsDNA amount produced by the cells on different surfaces over time (Fig. 5). After the 4-day incubation, no differences of the dsDNA amount between different groups were observed. The dsDNA amount produced by the cells on the Ti-6Al-4V increased and reached the plateau after the 8-day incubation. The dsDNA amount produced by the cells on the Ti-Ta-Nb disks exhibited no change after the 12-day incubation and began to increase till the 16-day incubation. The dsDNA amount produced by the cells on the sputtered nanoscale Ti-Ta-Nb coatings first decreased within the 12-day incubation and increased after the 16-day incubation. The cells on the Ti-6Al-4V disks produced a significantly greater dsDNA amount compared to the sputtered nanoscale Ti-Ta-Nb coatings ($P < .01$) and T-Ta-Nb disks ($P < .01$). The cells on the Ti-Ta-Nb disks produced significantly greater dsDNA compared to the sputtered nanoscale Ti-Ta-Nb coatings ($P < .01$).

Alkaline phosphatase (ALP) activity

The ALP specific activity by the cells on different surfaces over time. After the 4-day incubation, no differences of the ALP specific activity between different groups were observed (Fig. 6). The ALP specific activity on the Ti-6Al-4V decreased at first and then increased after the 16-day incubation. The ALP specific activity on the Ti-Ta-Nb disks decreased during the 16-day incubation. The cells on the sputtered nanoscale Ti-Ta-Nb coatings exhibited the greatest ALP specific activity after the 12-day incubation. The cells on the sputtered nanoscale Ti-Ta-Nb coatings exhibited significantly greater ALP specific activity when compared to the Ti-6Al-4V disks ($P < .01$) and Ti-Ta-Nb disks ($P < .01$). There was no significant difference between Ti-6Al-4V and Ti-Ta-Nb disks ($P = .33119$).

Total protein production assay

The total protein produced by the cells on different surfaces over time (Fig. 7). After the 4-day incubation, no differences of the total protein production between different groups were observed. The total protein produced by the cells on the

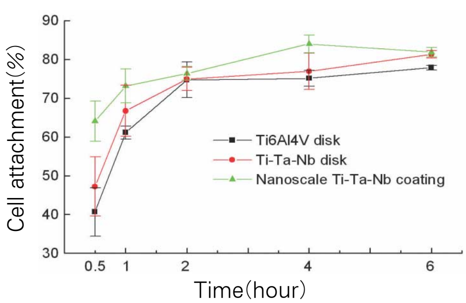

Fig. 3. Cell attachment kinetics of different surfaces.
(The sputtered nanoscale Ti-Ta-Nb coatings exhibited greater cell attachment compared to Ti-6Al-4V disks ($P < .01$) and Ti-Ta-Nb disks ($P < .05$). There were no significant differences between the Ti-Ta-Nb and Ti-6Al-4V disks.)

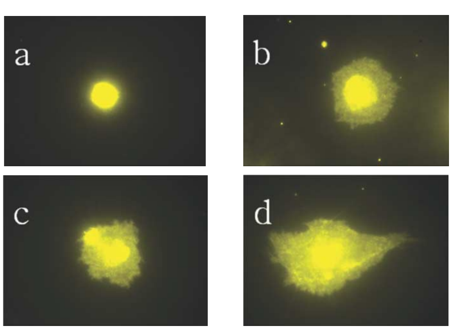

Fig. 4. Representative morphology change of the adherent cell on the samples over time. (a) 1 hour; (b) 2 hours; (c) 4 hours; and (d) 6 hours. Within the first hour, the adherent cell exhibited round shape. Within the first two and four hours, the adherent cell occupied larger and larger surface area and gradually changed to the elongated shape, suggesting the cell's continuing adhesion. Within the first six hours, the adherent cell exhibited the spindle shape and projected some visible filopodia, suggesting the start of spread.

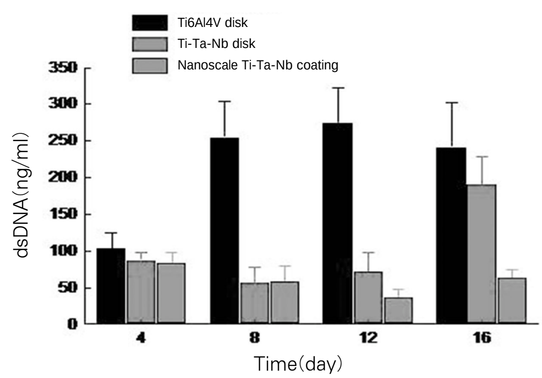

Fig. 5. dsDNA amount produced by the cells on different surfaces over time.
(The cells on the Ti-6Al-4V disks produced a significantly greater dsDNA amount compared to the sputtered nanoscale Ti-Ta-Nb coatings ($P < .01$) and T-Ta-Nb disks ($P < .01$))

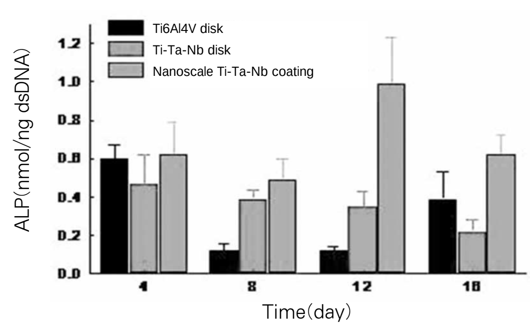

Fig. 6. ALP specific activity by the cells on different surfaces over time.
(The cells on the sputtered nanoscale Ti-Ta-Nb coatings exhibited significantly greater ALP specific activity when compared to the Ti-6Al-4V disks ($P < .01$) and Ti-Ta-Nb disks ($P < .01$))

Ti-6Al-4V decreased first and then increased after the 16-day incubation. The total protein produced by the cells on the Ti-Ta-Nb disks and sputtered nanoscale Ti-Ta-Nb coatings exhibited a peak after the 12-day incubation. The cells on the sputtered nanoscale Ti-Ta-Nb coatings exhibited significantly greater total protein production when compared to the Ti-6Al-4V disks ($P < .01$) and Ti-Ta-Nb disks ($P < .01$). The cells on the Ti-Ta-Nb disks produced significantly greater total protein compared to the Ti-6Al-4V disks ($P < .01$).

DISCUSSION

While modern metallic implants have been used with significant surgical success, less than ideal or variable responses are observed as delayed or failed osseointegration. These are often accompanied by infection or failure at the load-bearing bone-implant interface due to insufficient interface strength and / or intervening soft tissue. Approach to improve osseointegration includes modifying alloy composition and implant surface chemistry and topography and application of osseoconductive coating to implant surfaces. Each approach is striving to achieve rapid osseointegration and maximal strength of the bone-implant interface. The rationale for the newly developed Ti-Ta-Nb alloy grew out of the desire to avoid the use of vanadium and aluminum. In addition, recently nanoscale metal has been reported to enhance osteoblast adhesion and function,[24] we attempted to optimize the bone cell response to the nanoscale newly developed Ti-Ta-Nb surfaces.

The goal of this study was to increase our knowledge of the early biological behavior of osteoblast precursor on Ti-Ta-Nb disks and its sputtered nanoscale coatings. In order to accomplish this, the Ti-Ta-Nb alloy was cast and the Ti-Ta-Nb coatings were applied using the radiofrequency sputter coating method and cast Ti-Ta-Nb target. The Ti-6Al-4V was used as controls. In this study, both the polished Ti-6Al-4V and Ti-Ta-Nb disks exhibited alpha-titanium crystal structures and microscale groove surface morphology. The sputtered Ti-Ta-Nb coatings consisted of dense nanoscale grains with alpha-Ti crystal structure. The Ti-Ta-Nb disks and their sputtered nanoscale coatings exhibited greater hydrophilicity and rougher surfaces compared to the Ti-6Al-4V disks.

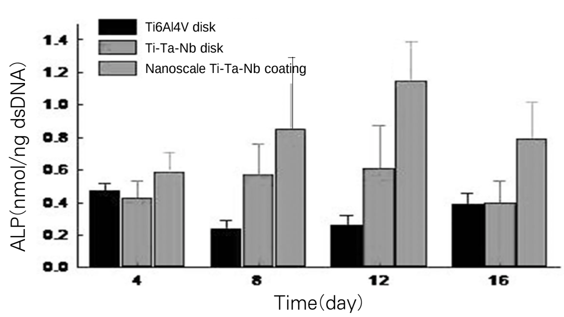

Fig. 7. Total protein produced by the cells on different surfaces over time. (The cells on the sputtered nanoscale Ti-Ta-Nb coatings exhibited greater total protein production when compared to the Ti-6Al-4V disks ($P < .01$) and Ti-Ta-Nb disks ($P < .01$))

Adhesion is an important cell function because it regulates a wide variety of processes such as cell growth, migration, cell differentiation, and extracellular matrix synthesis.[25,26] In this study, the percent adherence was determined using a coulter counter at different time points. The cell adhesion on all the surfaces exhibited a significant increase after the first two hours and reached a plateau after the first four hours. The sputtered nanoscale Ti-Ta-Nb coatings exhibited significantly greater cell adhesion compared to Ti-6Al-4V disks ($P < .01$) and Ti-Ta-Nb disks ($P < .05$). The enhancement of nanoscale surfaces is considered to be the result of the increase of grain boundary which provides the more cell adhesion binding sites.[24] In addition, the adherent cell morphology observation indicates that cells not only adhered well to the surfaces with the evidence of round shape after one hour adherence, but also spread well over time with the evidence of spindle shape with projected filopodia after six hour adherence.

In this study, we used the human mesenchymal cell, an osteoblast precursor cell line. In general, the precursor cells first experience division and then differentiation and mineralization.[27] At the early stage of differentiation, the early osteoblasts will express ALP. The mature osteoblasts produce extracellular matrix and then mineralization takes place with calcium phosphate deposition. The cell behavior following adherence was determined by examining dsDNA, ALP specific activity and total protein. dsDNA is used as a biomarker to evaluate the cell proliferation. It is supposed that as the ds DNA amount gets higher, the cell number increases. The dsDNA results show that the cells on the Ti-6Al-4V continued to proliferate during the first 8-day incubation and remained constant in the rest period of incubation, but the cells on the Ti-Ta-Nb disks and sputtered nanoscale Ti-Ta-Nb coatings did not exhibit proliferation except the Ti-Ta-Nb disks after the 16-day incubation. There were greater number of cells on the Ti-6Al-4V disks compared to the sputtered nanoscale Ti-Ta-Nb coatings ($P < .01$) and Ti-Ta-Nb disks ($P < .01$). Our results suggest that the precursor cells on the Ti-6Al-4V disks experienced a longer period of proliferation and a significant increase in cell number compared with the precursors on the Ti-Ta-Nb disks and sputtered nanoscale Ti-Ta-Nb coatings.

In terms of osteoblast differentiation, the results from the ALP specific activity show that the cells on the sputtered nanoscale Ti-Ta-Nb coatings significantly enhanced osteoblast differentiation when compared to the Ti-6Al-4V disks and Ti-Ta-Nb disks. There was no significant difference between Ti-6Al-4V and Ti-Ta-Nb disks. In addition to osteoblast differentiation, the interaction between the extracellular matrix and the osteoblast is essential for bone formation. Total protein is used to characterize the extracellular matrix formation. The results from total protein production suggest that both the sputtered nanoscale Ti-Ta-Nb coatings and Ti-Ta-Nb disks support significantly greater extracellular matrix formation compared to the Ti-6Al-4V disks. The reason that Ti-Ta-Nb alloy and its nanoscale coatings enhance osteoblast differentiation and extracellular matrix formation is probably due to the greater hydrophilicity and rougher surface as well as tantalum and niobium elements. We will continue the biological evaluation for the newly developed Ti-Ta-Nb alloys.

CONCLUSIONS

In this study, the newly developed Ti-Ta-Nb alloy has been cast and its nanoscale coating has been sputtered. The Ti-6Al-4V was used as controls. The three materials have been characterized using XRD, SEM, contact angle and surface roughness. HEPM cell was used to evaluate the osteoblast precursor response to the developed materials, including cell adhesion, proliferation and differentiation. The sputtered Ti-Ta-Nb coatings consisted of dense nanoscale grains in the range of 30 to 100 nm with alpha-Ti crystal structure. The Ti-Ta-Nb disks and their sputtered nanoscale coatings exhibited greater hydrophilicity and rougher surfaces compared to the Ti-6Al-4V disks. The sputtered nanoscale Ti-Ta-Nb coatings exhibited greater cell attachment compared to Ti-6Al-4V and Ti-Ta-Nb disks. The cells on Ti-6Al-4V disks exhibited significantly greater dsDNA amount compared to Ti-Ta-Nb disks and their sputtered nanoscale coatings during the 16-day incubation, suggesting higher cell proliferation on Ti-6Al-4V disks. Nanoscale Ti-Ta-Nb coatings exhibited greater ALP specific activity and total protein production compared to the other 2 groups, suggesting higher osteoblast differentiation and extracellular matrix production. In summary, Ti-Ta-Nb alloy and its sputtered nanoscale coating exhibits equivalent and better biological properties compared to Ti-6Al-4V alloy, suggesting their promising application in dentistry and orthopedics.

REFERENCES

1. Albrektsson T, Jacobsson M. Bone-metal interface in osseointegration. J Prosthet Dent 1987;57:597-607.
2. Kasemo B. Biocompatibility of titanium implants: surface science aspects. J Prosthet Dent 1983;49:832-7.
3. Linter CM. Neuropsychiatric aspects of trace elements. Br J Hosp Med 1985;34:361-5.
4. Srinivasan DP. Trace elements in psychiatric illness. Br J Hosp Med 1984;32:77-9.
5. Levine S. The management of resistant depression. Acta Psychiatr Belg 1986;86:141-51.
6. Li SJ, Niinomi M, Akahori T, Kasuga T, Yang R, Hao YL. Fatigue characteristics of bioactive glass-ceramic-coated Ti-29Nb-13Ta-4.6Zr for biomedical application. Biomaterials 2004;25:3369-78.
7. Niinomi M. Fatigue performance and cyto-toxicity of low rigidity titanium alloy, Ti-29Nb-13Ta-4.6Zr. Biomaterials 2003;24:2673-83.
8. Black J. Biological performance of tantalum. Clin Mater 1994;16:167-73.
9. Meenaghan MA, Natiella JR, Moresi JL, Flynn HE, Wirth JE, Baier RE. Tissue response to surface-treated tantalum implants: preliminary observations in primates. J Biomed Mater Res 1979;13:631-43.
10. Cohen R. A porous tantalum trabecular metal: basic science. Am J Orthop 2002;31:216-7.
11. Limberger F, Lenz E. Biological evaluation of In-Ceram-ceramics compared to cobalt-base-alloys and the metals titanium, tantalum and niobium in animal experiments [Article in German]. Dtsch Stomatol 1991;41:407-10.
12. Johansson CB, Hansson HA, Albrektsson T. Qualitative interfacial study between bone and tantalum, niobium or commercially pure titanium. Biomaterials 1990;11:277-80.
13. Breme J, Wadewitz V. Comparison of titanium-tantalum and titanium-niobium alloys for application as dental implants. Int J Oral Maxillofac Implants 1989;4:113-8.
14. Zitter H, Plenk H Jr. The electrochemical behavior of metallic implant materials as an indicator of their biocompatibility. J Biomed Mater Res 1987;21:881-96.
15. Rabenseifner L, Küsswetter W, Wünsch PH, Schwab M. Is fracture healing in the presence of biocompatible implant materials tantalum and niobium different in comparison to steel implants?[Article in German]. Z Orthop Ihre Grenzgeb 1984;122:349-55.
16. Fontaine AB, Koelling K, Passos SD, Cearlock J, Hoffman R, Spigos DG. Polymeric surface modifications of tantalum stents. J Endovasc Surg 1996;3:276-83.
17. Tepe G, Duda SH, Hanke H, Schulze S, Hagmeier S, Bruck B, Schott U, Betz E, Schmahl FW, Claussen CD. Covered stents for prevention of restenosis. Experimental and clinical results with different stent designs. Invest Radiol 1996;31:223-9.
18. Crochet D, Grossetête R, Bach-Lijour B, Sagan C, Lecomte E, Leurent B, Brunel P, Le Nihouannen JC. Plasma treatment effects on the tantalum Strecker stent implanted in femoral arteries of sheep. Cardiovasc Intervent Radiol 1994;17:285-91.
19. Brumme S, Löwicke G, Knöfler W. The use of tantalum wire as a suture material. [German] Z Exp Chir Transplant Kunstliche Organe 1989;22:308-13.
20. Shimko DA, Shimko VF, Sander EA, Dickson KF, Nauman EA. Effect of porosity on the fluid flow characteristics and mechanical properties of tantalum scaffolds. J Biomed Mater Res B Appl Biomater 2005;73:315-24.
21. Zardiackas LD, Parsell DE, Dillon LD, Mitchell DW, Nunnery LA, Poggie R. Structure, metallurgy, and mechanical properties of a porous tantalum foam. J Biomed Mater Res 2001;58:180-7.
22. Hacking SA, Bobyn JD, Toh K, Tanzer M, Krygier JJ. Fibrous tissue ingrowth and attachment to porous tantalum. J Biomed Mater Res 2000;52:631-8.
23. Bagley J, Rosenzweig M, Marks DF, Pykett MJ. Extended culture of multipotent hematopoietic progenitors without cytokine augmentation in a novel three-dimensional device. Exp Hematol 1999;27:496-504.
24. Webster TJ, Siegel RW, Bizios R. Osteoblast adhesion on nanophase ceramics. Biomaterials 1999;20:1221-7.
25. Shah AK, Sinha RK, Hickok NJ, Tuan RS. High-resolution morphometric analysis of human osteoblastic cell adhesion on clinically relevant orthopedic alloys. Bone 1999;24:499-506.
26. Berube P, Yang Y, Carnes DL, Stover RE, Boland EJ, Ong JL. The effect of sputtered calcium phosphate coatings of different crystallinity on osteoblast differentiation. J Periodontol 2005;76:1697-709.
27. Kartsogiannis V, Ng KW. Cell lines and primary cell cultures in the study of bone cell biology. Mol Cell Endocrinol 2004;228:79-102.